Ocean Dynamics (2019) 69:1239–1251
https://doi.org/10.1007/s10236-019-01293-z

Characteristics of ocean waves off Fortaleza, CE, Brazil, extracted from 1-year deep-water measured data

Rogério Neder Candella[1]

Received: 26 December 2018 / Accepted: 21 July 2019 / Published online: 20 August 2019

Abstract
One year of deep-water wave hourly records collected by a buoy deployed off Ceará state, northeastern Brazilian coast, were used to estimate some regional wave climate characteristics and annual cycles. Waves generated by four wind sources were identified. Southeastern direction showed to be the most effective, especially in the period from June to November due to southeast trade winds system intensification. Several dispersive arrivals of north Atlantic swell were recorded, and their generation zones were identified, which allows determining the region of main sources of these northern waves. Analysis of sea storms showed that although most of them had southeast direction, they could also come from the north. These northern storms sometimes are highly energetic, leading to damage in coastal structures. Only 37 records in the analyzed dataset around 0.4% of the total contained rogue waves. Although the number of occurrences of rogue waves was small, all of them were higher than 2.5 m.

Keywords Wind wave climate · Brazilian northeast region · North Atlantic swell · Storms characteristics

1 Introduction

Waves are the main form of energy transport in the ocean and the primary agent in coastal sediment dynamics. Thus, the knowledge of their characteristics and cycles is fundamental for better understanding coastal dynamics.

Nearly one third of the Brazilian coast, northern Cabo do Calcanhar (RN, approximately5°S; 35°W), is facing northeast, and due to its geographical position, it is directly exposed to trade winds, which drive the main components of the local wave climate.

Nevertheless, it is seasonally hit by long-traveled swell originated by storms in the north hemisphere. Branco (2005) showed that these waves from north have a strong seasonality with maximum in austral summer and spring. In addition, they can be highly destructive, causing damages in many places including Fernando de Noronha Island, as shown by the examples of newspaper headlines attached (Appendix).

This constant wave action drives a strong westward sediment transport in the region (Bandeira et al. 1990), and it has been highly affected by human interventions leading to intense erosion in places like Pontal de Maceió (Morais et al. 2008), Fortaleza waterfront (Silva et al. 2011), Mucuripe (Paula 2012), Pecém (Magini et al. 2013), Pacheco and Tabuba (Mororó et al. 2015), and Caucaia (Façanha et al. 2017).

There is a lack in wave measurements along Brazilian coast, and most of the existing ones are related to engineering purposes with short duration and shallow water deployment. In the northeast region, many studies were carried out on Ceará State coast (Fig. 1). Melo and Alves (1993) based their work on visual observations, while many other authors used wave measurements related to harbor construction, like Mucuripe and Pecém (Melo et al. 1995; Fisch 2008; Silva et al. 2011; Farias and Souza 2012).

However, these data were collected in typically 20 m depth. As the bathymetry of the region is characterized by a mild slope, deep waters were only found far from the coast (Fisch 2008). In this way, the direction of propagation of long waves in these measurements was altered by the bottom.

Within the framework of the National Buoy Plan—Plano Nacional de Boias, PNBOIA—conducted by the Brazilian Navy, an Axys 3M buoy (Argos ID: 146448; WMO ID:

This article is part of the Topical Collection on the *International Conference of Marine Science ICMS2018, the 3rd Latin American Symposium on Water Waves (LatWaves 2018), Medellin, Colombia, 19-23 November 2018 and the XVIII National Seminar on Marine Sciences and Technologies (SENALMAR), Barranquilla, Colombia 22-25 October 2019*

Responsible Editor: Alejandro Orfila

✉ Rogério Neder Candella
r.candella@marinha.mar.br; rcandella@gmail.com

[1] Instituto de Estudos do Mar Almirante Paulo Moreira, Rua Kioto 253, Arraial do Cabo, RJ 28930-000, Brazil

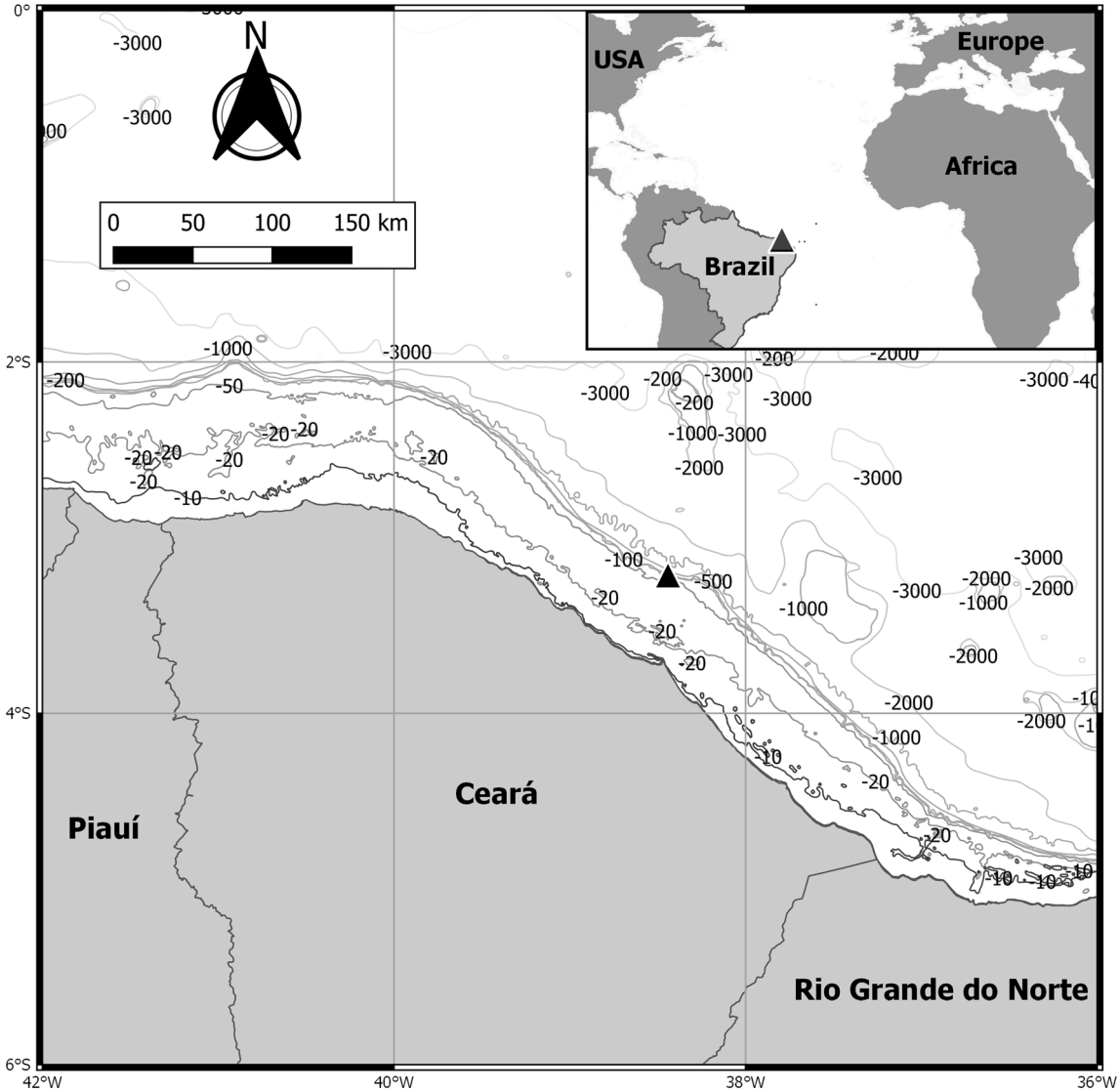

Fig. 1 Map of the northeastern Brazilian coast showing location of deployment of the PNBOIA buoy, off Ceará littoral. The deployment was at a depth of 200 m

31229) was deployed off Ceará coast, at coordinates 3.21°S; 38.44°W, 200 m depth, (Fig. 1) remaining operational from late October 2016 to early December 2017. Data recorded by this buoy were used in this work to estimate annual cycle and characteristics of the waves in the region.

2 Data description

Analyses were carried out from December 1, 2016, to November 30, 2017, and records had hourly sampling frequency. As heavy-north-east raw data were not available, the following statistical parameters processed by the buoy internal software were used:

- Significant wave height (Hs). Both definitions for significant wave height were available. $H_{1/3}$ is calculated in the time domain and represents the average of the highest 1/3 of the waves (Young 1999). However, the definition in the frequency domain (Hm0) was chosen. Following Young (1999), the value of Hm0 is four times the square root of the area under the spectral curve. Generally, their values are similar, but Hm0 can also be obtained by numerical modeling, which turns future comparisons with numerical modeling results easier
- Maximum wave height (Hmax), the largest wave height of the record
- Peak period (Tp), the most energetic wave period of the spectrum

Table 1 Sea state parameters of each forcing wind at Ceará coast. DANH means dispersive arrivals from the North Hemisphere

		Max Hs (m)	Period range (s)	Direction range
1	Local wind sea	1.1	2.0–5.0	NW to ESE
2	SE trade wind sea (SETW)	2.0	5.0–8.03	E to SE
3	NE trade wind sea (NETW)	1.1	8.03–11.2	N to NE
4	DANH	2.8	11.2–20.0	NW to NE

– Mean wave direction (Dm), computed by averaging the direction over all frequencies with the weighting function S(f)

Directional spectra processed by internal software of the buoy were also used.

Mean wave direction sometimes does not give clear information, especially under crossing wave systems condition. To overcome this problem, two additional parameters were extracted from directional spectra. The first one is peak direction (Dp), direction associated to peak period. The second is the most energetic direction of spectra given by

$$De\,(\theta) = \int_0^{0.64} E(f,\theta)\,\mathrm{df} \tag{1}$$

In the wave storms analysis, mean values were calculated for each variable. For example, mean Hm0 for each storm is given by

$$\overline{Hm0} = \frac{1}{n}\sum_{i=1}^{n} Hm0_i \tag{2}$$

where n is the number of records or hours in a storm. Analogous averages were taken for maximum wave high (Hmax), peak period (Tp), and peak direction (Dp). Although it is not usual to calculate average for direction, in this case, the standard deviation is very small, that is, the values of the directions are close to each other, turning the operation valid.

Characteristics of wind in the region were discussed by many authors, as Fisch (2008) or Camelo et al. (2008), for example, and will not be included herein.

3 Results

3.1 Statistical analyses and annual cycles

Waves arriving to the Ceará coast can have five main generation sources. First and more constant are those forced by southeast trade winds, followed by waves generated by northeast trade winds. Furthermore, there are the northern long-distance generated swell and the local generated wind sea. There are also waves generated by atmospheric African eastern disturbs, but they are very small when compared to local wave regime (Innocentini et al. 2005).

Fisch (2008) analyzed a 5-year wave time series and related sea states based on significant wave height, peak period, and direction to generating winds as shown in Table 1, where DANH means dispersive arrivals from the North Hemisphere.

Peak period and peak direction relation obtained in this work (Fig. 2) approaches qualitatively to sea state classes cited by that author, whose class limits are marked by rectangles and indicated by numbers. The only remarkable difference is that, in the dataset analyzed in this work, waves with periods in the range 5 to 11.2 s had directions more widely distributed, from 0 to 150°. Yet according to Fisch (2008), winds from northwest to north in the area represent only around 1.5% of the total and are generally short-lived and low intensity. So, local generated short period waves from these directions are not expected to be frequent. Anyway, there is no clear reason for their complete absence in the results obtained. It can be assumed that the differences are related to the nearest or farthest deployment position from the coast, refraction effects or operational range of wave periods of the equipment.

Hs (upper panel) and Hmax (lower panel) data time series used here can be seen in Fig. 3. Hm0 average for the whole period was 1.78 ± 0.39 m. The maximum value (3.61 m) occurred at September 19, 06:00 GMT. Hmax mean was 2.71 ± 0.66 m, and the extreme wave was recorded at July 30, 09:00 GMT, with 5.87 m height, associated to 2.65 m Hm0. Both mean values are much greater than those found by Fisch (2008) and Silva et al. (2011). A remarkable difference in the variance of both series can be seen from June/July onwards. An analogous behavior is also observed in the other parameters like Tp and Dm, as will be showed ahead, and these changes can be related to the intensification of the SE trade winds.

Following Dean (1990), Abnormality Index (AI) is the ratio between H and Hm0, where H is the height of any individual wave of the record. To be considered a rogue wave, AI must be greater than 2, or $H \geq 2 \cdot Hm0$. As raw data was not available, in this study, AI is given by AI = Hmax/Hs. Linear regression adjusted to data showed the relation

$$\mathrm{Hmax} = 1.56\text{*Hm0} - 0.07,$$

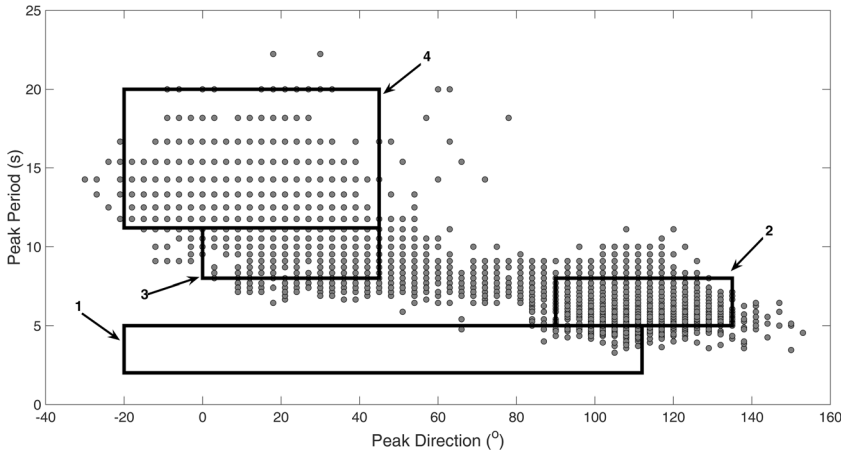

Fig. 2 Peak direction and peak period scattering diagram showing different sea state classes according to their forcing winds. Boxes are the limit of each class as cited by Fisch (2008). Both distributions approach qualitatively, except for high-frequency waves related to local wind, and there is no clear reason for this difference

very similar to characteristic south/southeastern regions (Candella 2016). Figure 4 shows the dispersion diagram Hm0 × Hmax, as well as the linear adjustment and limit to rogue waves (Hmax ≥ 2Hs).

Hm0 and Hmax histograms can be seen in Fig. 5 a and b, respectively. Their modal values were 1.4 and 2.4 m.

Peak period ranged from 3.3 to 22.2 s, with mean equals to 8.7 ± 3.2 s and modal value 6 s. Half of the records showed Tp shorter than 6 s, while 75% of records were shorter than 10 s, and 99% of them were shorter than 17 s. Figure 6 a displays Tp evolution along the year. A change in variance is noticeable from June onwards, due to the presence of the shorter waves generated by SE trade wind intensification. Probability distribution (Fig. 6b) exhibits a concentration around 6 s, but there is also the presence of a significant tail in the low-frequency band. Longer periods are associated to long-distance generate northern waves.

Due to the geographic position of the coast, wave directions vary from NW to SE or 344° (− 16°) to 145°. Figure 7 a shows peak direction time series. Analogously to Tp, there is a clear change in the series variance around June, with a tendency towards southeast direction associated to waves formed by intensification of SE trade winds. A clear bimodal distribution is shown in Fig. 7 b, with main peak associated to SE direction and a secondary one related to waves formed by NE trade winds as well as long-distance generated northern waves.

Normalized energy contours of Dp × Tp shown in Fig. 8 clearly evidence an annual cycle. From June to November, there is a predominance of waves from the southeast associated to short periods. In December and January, both SE and North/Northeast waves are present, with higher periods linked to N/NE waves. In the following months, namely February, March, and April, peak direction tends to be only N or NE, while May seems to be the transitional month, with waves from all main directions.

Probability distribution of the most energetic direction (Fig. 9) corroborates the above affirmative exhibiting a quite similar monthly variation. From June to November, most of

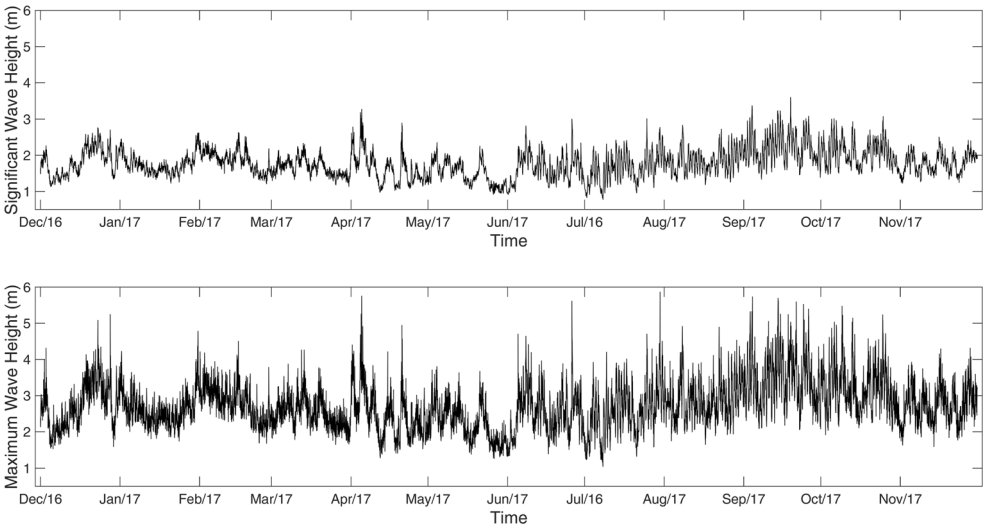

Fig. 3 Hm0 (upper panel) and Hmax (lower panel) time series for whole period. Both mean and maximum values for both parameters are much greater than those found in the previous works of Fisch (2008) and Silva et al. (2011). There is a noticeable change in the variance of both series from June/July onwards related to the intensification of the SE trade winds

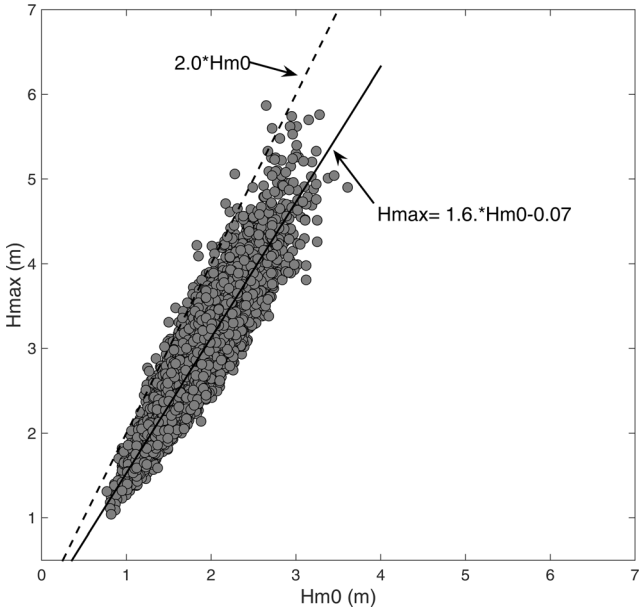

Fig. 4 Hm0 to Hmax correlation for the whole data. Solid line is the linear regression adjusted to data, and the coefficient of the linear regression is close to the mean value found by Candella (2016) to Brazilian south and southeast regions. Dashed line is the limit to rogue wave relation (Hmax ≥ 2·Hm0)

the energy is concentrated in southeast direction, whereas in the other months, energy coming from N/NE is also present, sometimes as the most significant energy source.

3.2 Dispersive arrivals

Deep-water waves are dispersive, meaning that longer waves travel faster than shorter ones. Then, if the generation zone is far enough, there will be a dispersive arrival, characterized by gradual decrease of the peak period (Tp).

Starting from the well-known dispersion equation for deep-water waves:

$$\sigma^2 = g \cdot k \tag{3}$$

where $\sigma = \frac{2\pi}{T}$ and T is the period of the wave, g is the gravity acceleration and $k = \frac{2\pi}{L}$, k is the wave number and L is the wave length, the distance X from the wave generation zone can be determined by

$$X = \frac{g\Delta t}{4\pi\Delta f} \tag{4}$$

where X is given in meters, Δt is the propagation time of the waves, and $\Delta f$is variation of the frequencies, as first described by Munk et al. (1963).

Melo and Alves (1993), Melo et al. (1995), Fisch (2008) and Farias and Souza (2012) had already cited dispersive arrivals of waves to Ceará coast, but their analyses were based on visual and/or intermediary water measurements.

Still following linear theory, wave length in deep water approximation can be expressed as $L = 1.56 \cdot T^2$, where L is the wave length and T the period. In practice, waves are in deep water if $h = L/4$ (WMO 1988). As the longer period found was 22.2 s, all waves can be considered deep-water waves, and it can be assumed that the propagation direction was not effectively influenced by the bottom.

Using the distance X, the deep water group velocity $\left(Cg = \frac{c}{2} = 0.78 \cdot T^2\right)$ and the direction of the first waves, it

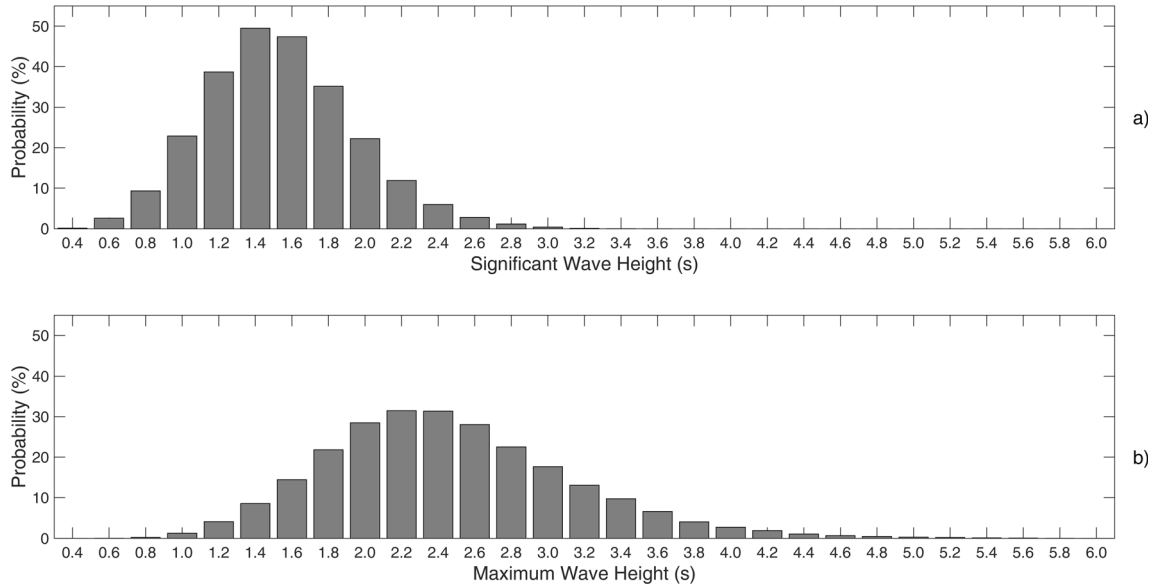

Fig. 5 Hm0 (**a**) and Hmax (**b**) histograms for the whole data. The modal values for both distributions show that the sea conditions are not severe most of the time

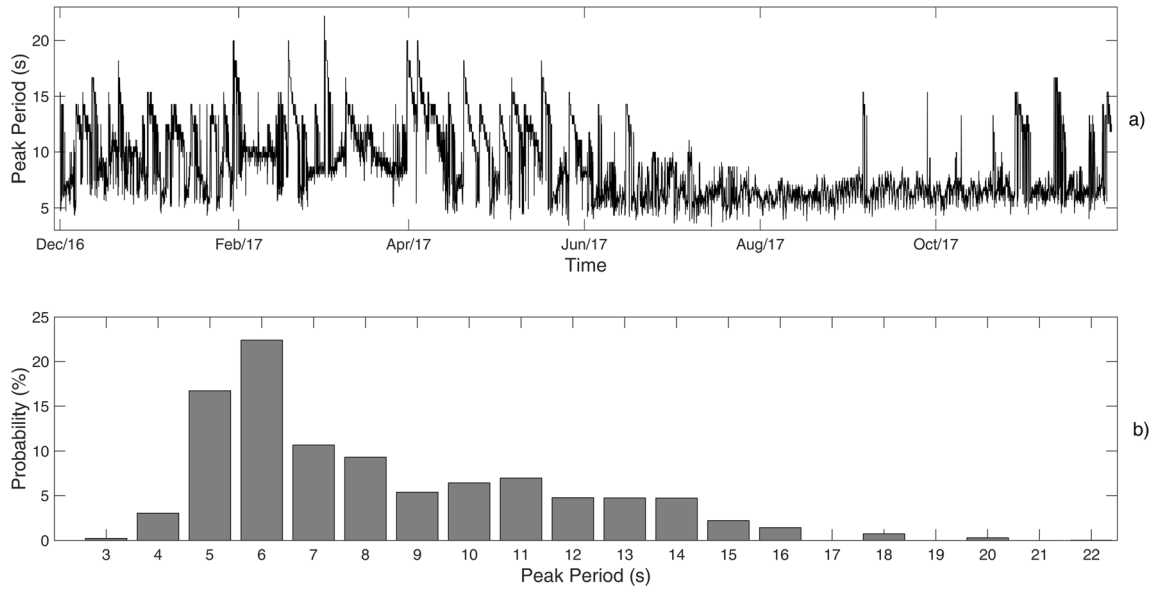

Fig. 6 Tp time series (**a**) showing noticeable change in variance from June onward. The probability distribution (**b**) shows a pronounced peak around 6 s, but a significant tail in the low frequency band also can be seen

is possible to estimate the generation zone of each event by tracing arcs of great circle.

All northern waves with Tp longer than 12 s seem to arrive at Brazilian North coast in a dispersive way, but sometimes, the gradual decrease on peak period is not so clear due to interference of other wave systems. Table 2 shows some characteristics of 12 arrivals that could be clearly identified. In this table, **Ti** means the peak period of the arrival beginning, **Tf** is the ending peak period, **Dist** is the estimated distance to generation zone, **Direc** is the peak direction of the first waves, **Prop. Time** is the propagation time, **Max** and **Mean Hs** are maximum and average significant wave height of the event, and **Max** and **Mean Hmax** are analogous to the maximum and the mean height of highest individual waves.

Generation zones were determined based on Eq. 3 and are shown in Fig. 10. No seasonality pattern related to positioning of these zones was found.

Some of these dispersive arrivals produced heavy wave conditions, especially those in April 4 and May 2. Significant waves during these events were almost four standard deviations higher than mean Hm0.

According to the information obtained from the National Hurricane Center accessed in September 2018 at <https://www.nhc.noaa.gov/data/>, the generation area of the last

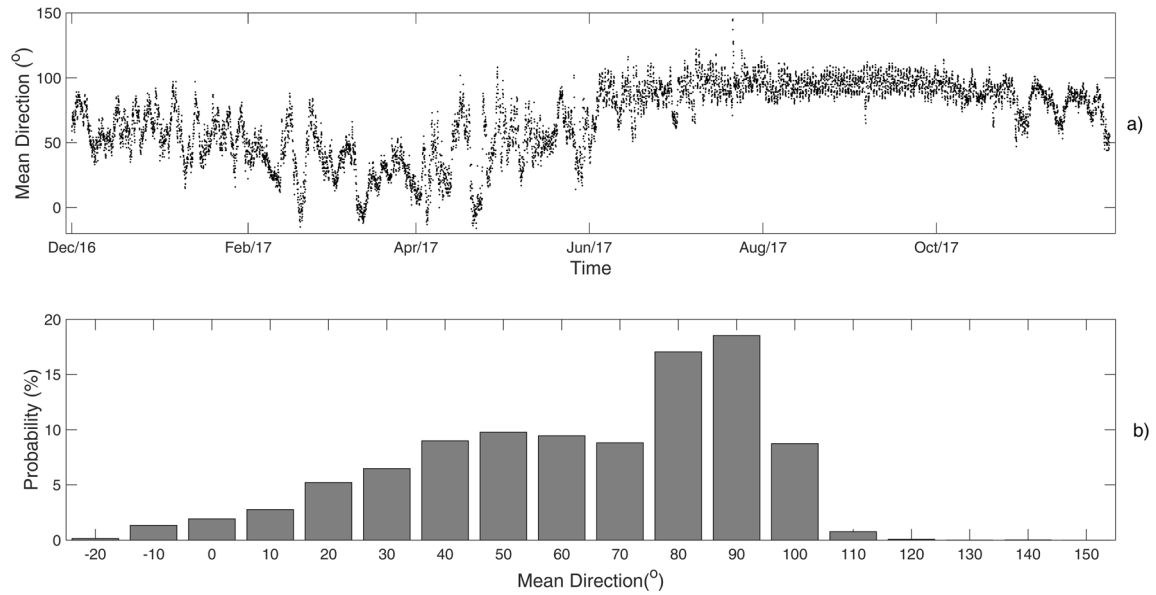

Fig. 7 Peak direction time series (**a**) and probability distribution (**b**). Analogously to TP, there is a clear change in the variance from June onward and a bimodal probability distribution, with peaks in SE and N/NE directions

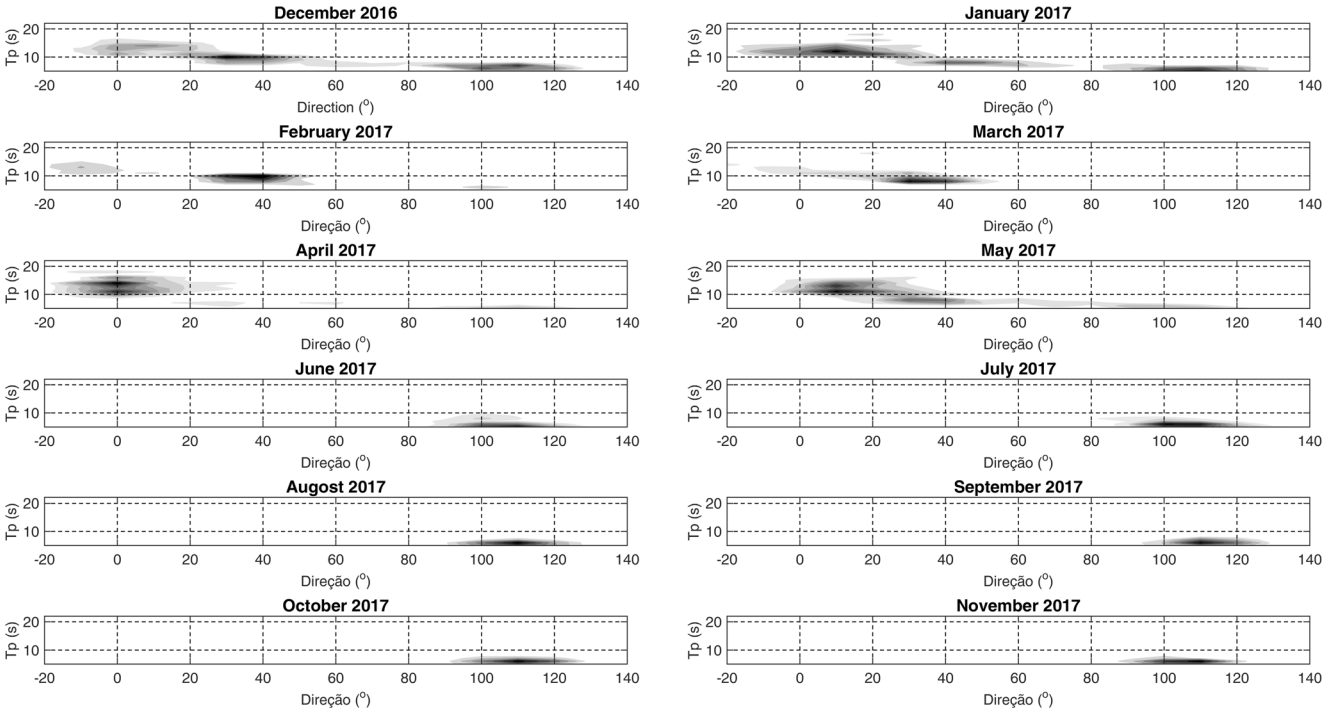

Fig. 8 Normalized energy contours for peak direction (Dp) and peak period (Tp) showing annual cycle of energy distribution. From June to November, short period waves from SE are predominant. In other months, longer period waves from N/NE are the main source of energy

dispersive event listed in Table 3 is close to the trajectory of hurricane Irma (Fig. 10). Occhi (2003) cited that the larger waves travel ahead of the hurricane as swell, and peak periods longer than 15 s can be generated depending on severity of sea state, like those observed in hurricane Gloria. In this case, peak direction of the waves was different from the trajectory path of the hurricane, and no references could be found in the literature relating wave dispersive arrivals to hurricanes.

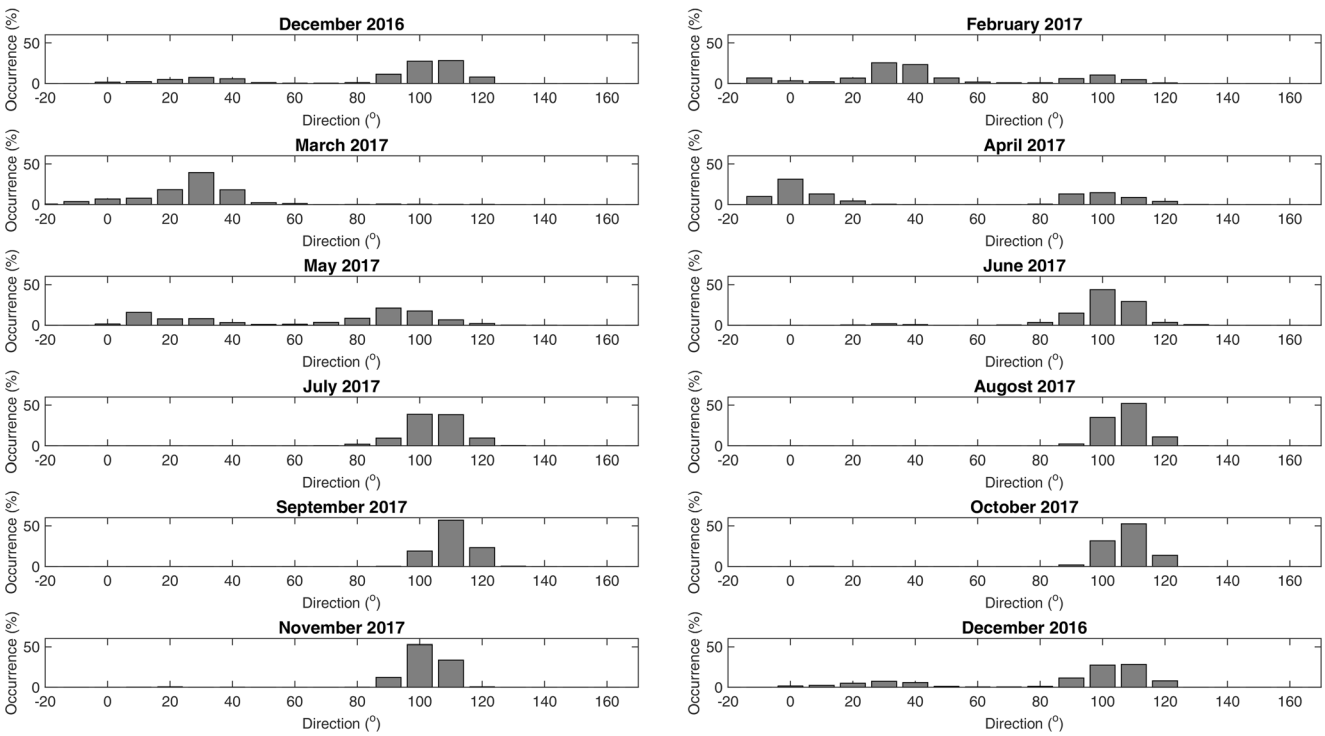

Fig. 9 Monthly most energetic wave direction histogram. Distribution pattern corroborates the annual cycle evidenced by monthly Dp × Tp contours, exhibiting a quite similar variation

Table 2 Waves characteristics of dispersal arrivals that could be identified in data set

Date	**Ti** (s)	**Tf** (s)	**Dist** (km)	**Direc** (°)	**Prop. Time** (h)	**Max Hs** (m)	**Mean Hs** (m)	**Max Hmax** (m)	**Mean Hmax** (m)
Dec 06, 2016	14.3	11.1	5292	18	130	1.66	1.44	2.47	2.01
Dec 08, 2016	15.4	11.8	5527	0	130	1.68	1.44	2.82	1.57
Dec 21, 2016	18.2	13.3	5964	351	120	2.62	2.27	4.28	3.45
Feb 18, 2017	20.0	13.3	5127	0	90	2.53	2.10	3.55	2.91
Mar 02, 2017	22.2	14.3	6205	18	100	2.15	1.74	3.26	2.54
Mar 31, 2017	20.0	11.8	7191	15	130	2.79	1.92	4.41	2.89
Apr 04, 2017	20.0	11.1	6093	354	110	3.28	2.26	5.76	3.33
Apr 20, 2017	18.2	9.1	5161	354	100	2.90	1.64	4.95	2.50
May 02, 2017	14.3	9.1	6112	21	150	3.26	1.76	3.81	2.64
May 26, 2017	15.4	11.1	5915	15	140	1.24	1.11	2.08	1.69
Jun 15, 2017	14.3	10.5	4215	15	110	1.88	1.49	2.72	2.16
Sep 05, 2017	15.4	11.8	2126	348	50	2.19	1.95	3.92	2.95

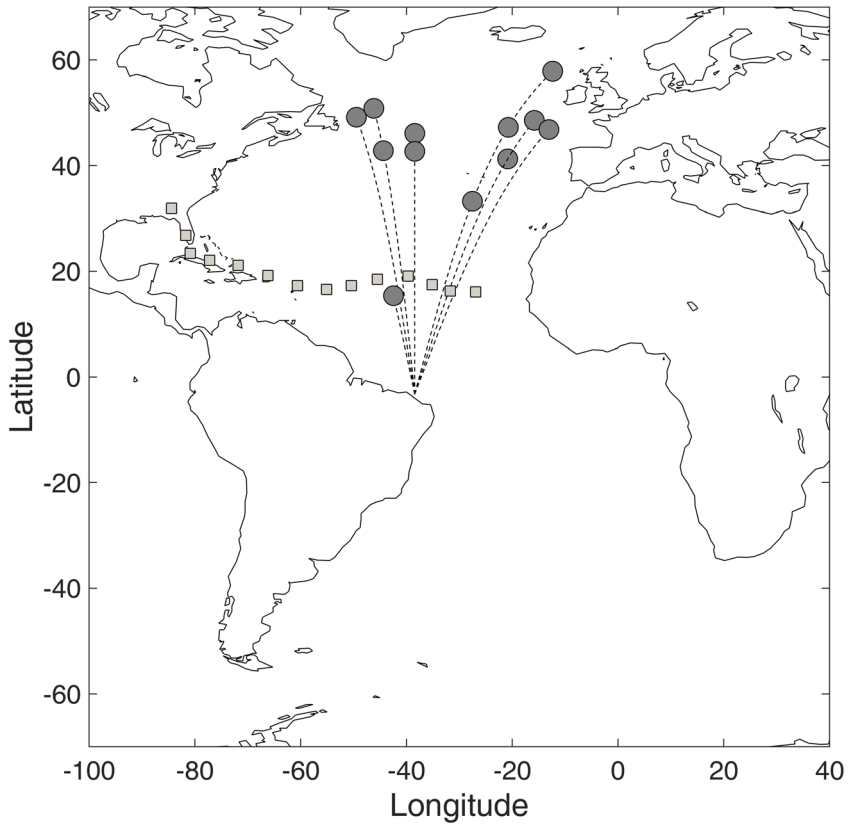

Fig. 10 Gray circles mark the location of the generation zones of dispersive arrival events measured in the Ceará coast in 2017. Dotted lines are arc of circles representing directions of propagation. Gray squares show hurricane Irma's trajectory from 2017, August 30, 00:00 UTM (rightmost point) to 2017, September 13, 00:00 UTM, proving that this atmospheric system was the forcing of the dispersive arrival event recorded

Table 3 Number of rogue waves in each month of the year

	Jan	Feb	Mar	Apr	May	Jun	Jul	Aug	Sep	Oct	Nov	Dec
Number of RW	1	2	3	4	5	3	5	5	4	0	3	0

NCEP Reanalysis sea level atmospheric pressure and wind at 10 m fields accessed at <https://www.esrl.noaa.gov/psd/data/gridded/data.ncep.reanalysis.surface.html> (not presented here) showed no other possible source for those waves in the North Atlantic.

3.3 Wave storms analysis

According to Boccotti (2000), a sea storm is a sequence of sea states in which significant wave height exceeds a threshold value. Here, a minimum duration was not defined, which means that a single record above the limit can be considered a storm. In addition, Hm0 cannot fall below this limit for more than 12 continuous hours to be considered as a part of the same storm, the same criterion adopted by Broccotti (2000).

Threshold limit (Hcrit) can be defined as an arbitrary value, for example 2.0 m, as adopted by Candella et al. (2008), or as a location-dependent wave height, as proposed by Broccotti (2000), where Hcrit equals 1.5 times $\overline{\mathrm{Hs}}$. This last criterion was adopted in this work, and as $\overline{Hm0} = 1.78\ m$, Hcrit = 2.67 m.

Forty events were classified as sea storm using the previously mentioned parameters. All storms occurred between April and December, although over 70% of them were concentrated in September (19 storms) and October (10 storms) (Fig. 11, upper panel). Most of storms had short duration. Only one event was longer than 12 h (Fig. 11, central panel) and 72.5% shorter than 6 h (Fig. 11, lower panel). Mean storm duration was approximately 5 h, ranging from 1 to 26 h.

Of the 40 wave storms detected, 37 had average direction southeast (more than 100°). The other three had north as mean direction (around 0°). As expected, the peak period related to northern waves were longer than those from SE direction (Fig. 12, left panel). On the other hand, although mean Hm0 from north were generally smaller than those from southeast (Fig. 12, central panel, gray circles), their maximum wave heights can be high enough to lead to the destructive episodes already mentioned (Fig. 12, right panel, gray circles).

A northern event occurred in April 20/21 showed mean Hm0 (2.50 m) smaller than Hcrit. It happens due to the presence of 2 records above Hcrit separated by less than 12 h. In this way, all points below the critical limit and between these two records were also considered as part of the storm (Fig. 13).

The strongest storm registered during the measurement period started at September 9, 2017, 02:00 GMT, and lasted for

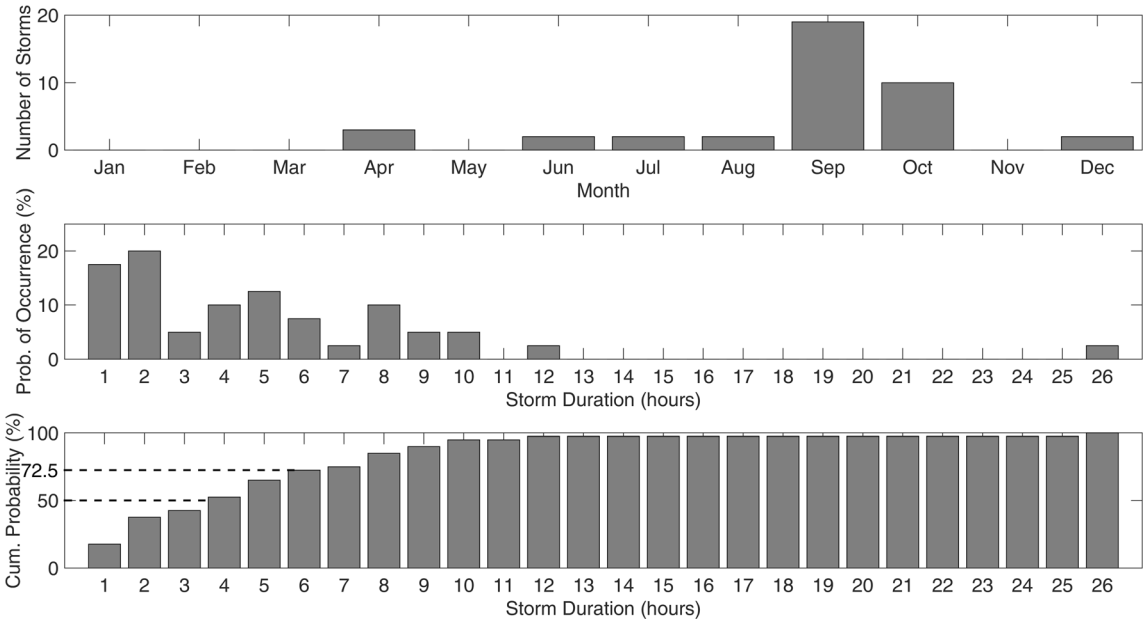

Fig. 11 Monthly distribution of storms (upper panel), storm duration probability distribution (central panel), and duration cumulative probability (lower panel) for the whole analyzed period. It is noticeable that more than 70% of occurrences have been concentrated between September and October, and the duration of storms is predominantly short in time, with 72.5% of the storms shorter than 6 h

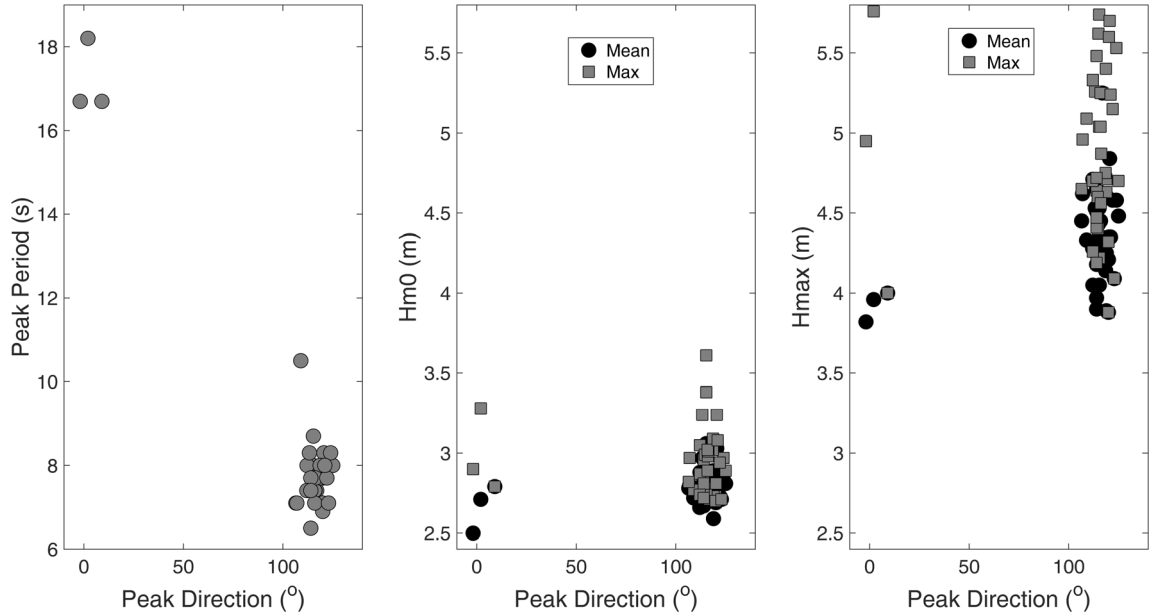

Fig. 12 Mean peak period (left panel), mean Hm0 (central panel, black circles), and mean maxima waves (right panel, black circles), in relation to mean peak direction for each sea storm. Gray squares in central and right panels represent the same relation to maxima values of each storm. The predominance of the storms with southeast mean direction is clear

10 h. Mean Hm0 was 3.06 m while mean Hmax was 4.53 m. Average peak direction was 115° and Tp ranged from 7.1 to 8.7 s.

3.4 Rogue waves

Rogue waves (RWs) are those with individual height greater than twice significant wave height of a record as defined by Dean (1990). They can appear in any sea state, wind sea or swell, shallow or deep water.

During the measurement period, 37 rogue waves were recorded. Figure 14 shows abnormality index time series, and rogue waves are those represented above the dashed line, marked with a gray circle. Visually, RWs seem to be more frequent between May and October, when wave peak direction starts trending to SE, and there is at least one RW for month, except in October and December (Table 3). However, as shown in Fig. 15a–d, the distribution of AI with other wave parameters presents no clear pattern, except that FW tended to occur when mean direction lies between NE and SE.

Rogue wave height varied from 2.51 m (AI = 2.04) to 5.87 (AI = 2.22). Maximum AI was registered in April 15, 2017 07:00 GMT, with Hmax = 4.22 m and Hs = 1.83 m, resulting in AI = 2.31. Directional spectrum of this record shows a wide frequency band, composed by a swell with peak period 14.3 s, from 60°, associated to

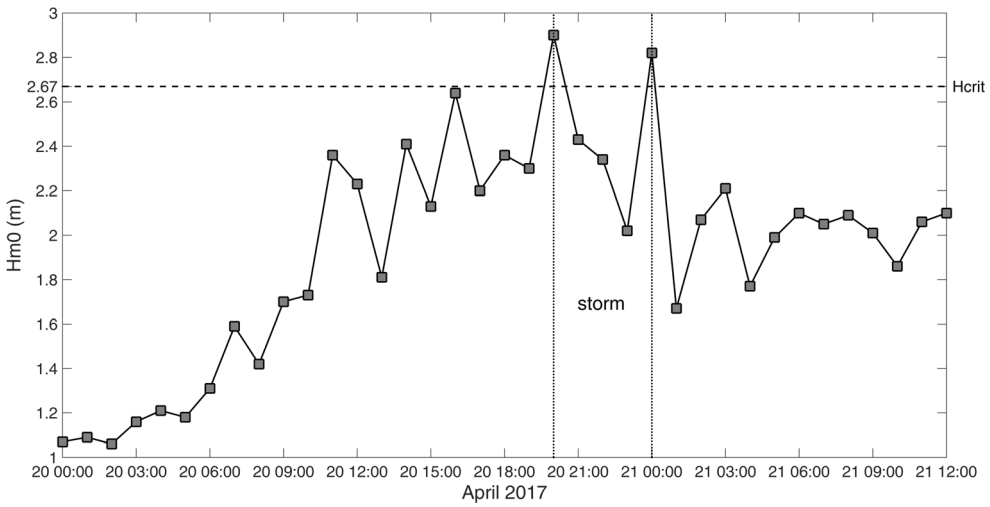

Fig. 13 Northern storm with 2 records above Hcrit separated for less than 12 h. All points below the critical limit and between these two records were also considered as part of the same storm

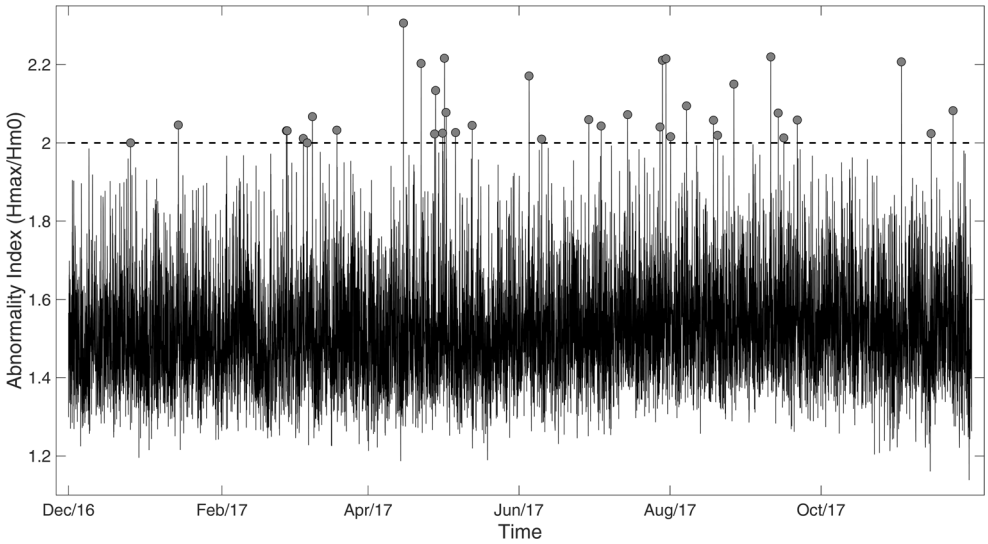

Fig. 14 Abnormality index time series for the whole period. Rogue waves lie above dashed line and are marked with a gray circle

a southeastern wind sea with periods ranging from about 5 to 7 s. The highest RW was also the highest individual wave measured during the whole period. It was associated to Hm0 = 2.65 m, mean direction of 109°, and Tp = 7.7 s, characterizing a typical sea state generated by SE trade winds.

4 Conclusions

Even though the analyzed time series was short for an accurate estimate of wave climate, the lack of continuous measurement in the region and the deep-water location of the buoy highlight its relevant to the knowledge of wave charcateristics in the South Atlantic Ocean.

In the analyzed period, waves off the Ceará coast showed a well marked seasonal behavior. From June to November, southeastern waves related to southeastern trade wind intensification are dominant. From December to May, the main waves came from northeast and north. Locally generated wind sea is present during the whole year, with characteristic short period, widely spread direction, and low height.

Mean significant wave height was 1.78 ± 0.39 m, with maximum value of 3.61 m. It is low if compared

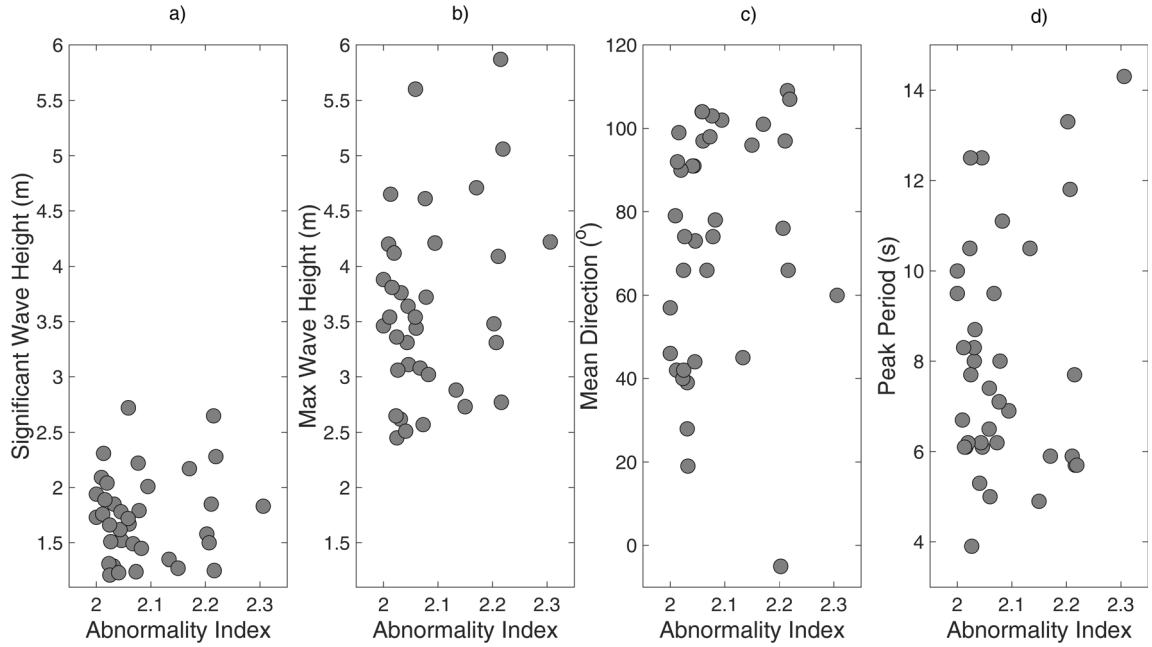

Fig. 15 Abnormality Index (AI) relation with Hs (**a**), Hmax (**b**), mean direction (**c**), and peak period (**d**) dispersion graphics for all the rogue waves detected. As can be seen, there is no striking pattern in the relationships between the parameters

to the Brazilian south coast, estimated as $\overline{Hm0}$≈2.20 m, but is close to the average Hm0 determined for Brazilian southeast region, around 1.90 m (Candella 2016). This result does not agree with those previously obtained by Silva et al. (2011), who found 1.35 m, 1.33 m, and 2.08 m for 1997, 2000, and 2001, respectively.

Hmax mean value was 2.71 ± 0.66 m, with extreme value 5.87 m. Again, it does not concur with Silva et al. (2011), but their Hmax results seemed to be strongly contaminated by spikes.

Range of peak period varied from 3.3 to 22.2 s. Shorter periods are related to localy generated wind sea, while Tp between 5 and 10 s is linked to southeastern waves. Waves with period longer than 8 s are associated to north and northeast direction. Half of the records showed Tp shorter than 6 s, 75% of them were shorter than 10 s, and 99% of the peak periods were shorter than 17 s.

Under non-rare conditions, long-distance generated swell with north direction may be high enough to cause severe damage to coastal structures, which has been constantly reported by Brazilian media. On some occasions within the measurement period, its significant wave height was more than 3 standard deviations above the Hm0 average. These waves always arrive in a dispersive way, with initial long periods.

Wave storms in the area have generally short duration, and almost all of them were shorther than 12 h. They tend to concentrate on September and October, with 37 of the 40 storms coming from the SE, and only on three occasions they had the north direction.

A low number of rogue waves could be identified in the records. Only 37 events were found in 8760 records, which leads to an occurrence of 0.4%. It is much smaller than that found in the south and southeast regions of Brazil (Candella 2016). However, all rogue waves found in the time series were higher than 2.5 m, and the highest rogue wave identified was also the highest of all waves measured throughout the period.

Acknowledgments The author would like to thank Dr. Luigi Cavaleri (ISMAR.CNR.IT) for his help to this work.

Appendix. Northern storms in Brazilian media.

01/03/2018.

http://g1.globo.com/ceara/cetv-2dicao/videos/v/ressaca-do-mar-causa-estragos-no-litoral-cearense/6543824/

31/03/2017.

http://g1.globo.com/ceara/cetv-2dicao/videos/v/com-ressaca-do-mar-ondas-no-litoral-de-fortaleza-chegam-a-25-metros/5768755/

06/08/2013.

http://g1.globo.com/ceara/bom-dia-ce/videos/v/veja-como-esta-a-ressaca-do-mar-em-fortaleza/2738415/

24/03/2013.

https://extra.globo.com/noticias/brasil/ressaca-causa-destruicao-em-fernando-de-noronha-no-ceara-483262.html

References

Bandeira JV, Araújo LC, Valle AB (1990) Emergency situation in the shoreline reach of an offshore oilfield pipeline and remedial measures. Trade Wind Sea. Conf., ASCE, pp 3171–3182

Boccotti P (2000) Wave mechanics for ocean engineering. Elsevier Science, New York

Branco FV (2005) Contribuições de Swell Gerado em Tempestades Distantes para o Clima de Ondas na Costa Brasileira. MSc Dissertation, IAG/USP, São Paulo, SP, Brasil.

Camelo HN, Carvalho PCM, Leal Junior JBV, Accioly Filho JBP (2008) Análise estatística da velocidade de vento do estado do Ceará. Rev Tecnol Fortaleza 29(2):211–223

Candella RN (2016) Rogue waves off the south/southeastern Brazilian coast. Nat Hazards 83:211–232. https://doi.org/10.1007/s11069-016-2312-2

Candella RN, Lomonaco DR, Leonardo M. Marques da Cruz LM, Ferreira RS (2008) Análises Preliminares das Características Regionais das Ondas ao Longo da Costa Brasileira Através de Modelagem Numérica. Congresso Brasileiro de Oceanografia, Fortaleza, CE

Dean R (1990) Freak waves: a possible explanation. In: Tørum A, Gudmestad OT (eds) Water wave kinematics. Kluwer Academic Publishers, Norwell, pp 609–612

Façanha MC, Di Ciero CD,Souza LA, Marino MTRD (2017) Erosão Costeira da Praia do Icaraí (Caucaia/Ce). XVI Simpósio de Geografia Física Aplicada - I Congresso Nacional de Oceanografia Física, Instituto de Geociências, UNICAMP, ISBN 978-85-85369-16-3, 2946–2952. https://doi.org/10.20396/sbgfa.v1i2017.2165

Farias EGG, Souza JMAC (2012) Chegada Dispersiva de Campos de Ondas Swell na Costa Oeste do Estado Ceará – Brasil. Arq Ciên Mar, Fortaleza 45(1):69–74

Fisch CI (2008) Caracterização do Clima de Ondas na Costa do Ceará. Dissertation. COPPE-UFRJ, Rio de Janeiro, Brazil, p 118

Innocentini V, Arantes FO, Ferreira RJ, Micheleto RG (2005) A Agitação Marítima no Litoral Nordeste do Brasil Associada aos Distúrbios Africanos de Leste. Revista Brasileira de Meteorologia 20(3):367–374

Magini C, Martins AHO, Pitombeira ES (2013) A Infraestrutura Portuária e suas Influências na Sedimentação Costeira na Vila do Pecém, Ceará, Brasil. Geociências 32(3):532–546

Melo FE, Alves JEGM (1993) Nota sobre a Chegada de Ondulações Longínquas à Costa Brasileira. Anais do X Simpósio Brasileiro de Recursos Hídricos, Vol. 5, ABRH, Gramado, RS, Brazil, pp 362–369

Melo FE, Alves JEGM, Jorden W, Zago F (1995) Instrumental confirmation of the arrival of north Alantic swell to the Ceará coast. Proceedings of the 4th International Conference on Coastal and Port Engineering in Developing Countries – COPEDEC IV, Rio de Janeiro, Brazil, pp 1984–1996

Morais JO, Pinheiro LS, Cavalcante AA, Paula DP, Silva RL (2008) Erosão Costeira em Praias Adjacentes às Desembocaduras Fluviais: O Caso de Pontal de Maceió, Ceará, Brasil. Revista da Gestão Costeira Integrada 8(2):61–76

Mororó EAA, da Silva RMN, Souto MVS, Duarte CR (2015) Análise de 22 anos (1991- 2013) da evolução costeira para a porção do litoral

cearense, a oeste da cidade de Fortaleza, por meio de imagens históricas da série Landsat. Anais XVII Simpósio Brasileiro de Sensoriamento Remoto - SBSR, INPE, João Pessoa-PB, Brasil

Munk WH, Miller GR, Snodgrass FE, Barber NF (1963) Directional recording of swell from distant storms. Phil Trans R Soc A 255: 505–584. https://doi.org/10.1098/rsta.1963.0011

Occhi MK (2003) Hurricane-generated seas. Elevier Ocean Engineering Book Series.140+xiv p

Paula DP (2012) Análise dos riscos de erosão costeira no litoral de Fortaleza em função da vulnerabilidade aos processos geogênicos e antropogénicos. Tese de doutoramento, Ciências do Mar (Gestão Costeira), Faculdade de Ciências e Tecnologia, Universidade do Algarve, Portugal

Silva AC, Façanha P, Bezerra C, Araujo A, Pitombeiras E (2011) Características das Ondas "Sea" e "Swell" Observadas no Litoral do Ceará-Brasil: Variabilidade Anual e Inter-Anual. Trop Oceanogr, Recife 39(2):123–132

Young LR (1999) Wind generated ocean waves. Elsevier Ocean engineering book Series. 288 + xvii p